P-07-207

Forsmark site investigation

Borehole KFM06A

Uniaxial compression test of intact rock containing sealed fractures

Lars Jacobsson, SP Technical Research Institute of Sweden

October 2007

Svensk Kärnbränslehantering AB
Swedish Nuclear Fuel
and Waste Management Co
Box 250, SE-101 24 Stockholm
Tel +46 8 459 84 00

ISSN 1651-4416
SKB P-07-207

Forsmark site investigation

Borehole KFM06A

Uniaxial compression test of intact rock containing sealed fractures

Lars Jacobsson, SP Technical Research Institute of Sweden

October 2007

Keywords: Rock mechanics, Uniaxial compression test, Elasticity parameters, Stress-strain curve, Sealed fractures, AP PF 400-04-121.

Abstract

Uniaxial compression tests with loading up to and just passing compressive failure were carried out on 6 water saturated specimens of intact rock containing sealed fracture networks from borehole KFM06A in Forsmark. The sampled rock type was medium grained granite. The cylindrical specimens were taken from drill cores at one depth level ranging between 325–330 m borehole length. The elastic properties, represented by Young's modulus and the Poisson ratio, and the uniaxial compressive strength were deduced from these tests. The wet density of the specimens was determined before the mechanical tests. The specimens were photographed before as well as after the mechanical testing.

The measured densities for the water saturated specimens were in the range 2,640–2,650 kg/m^3 yielding a mean value of 2,645 kg/m^3, whereas the peak values of the axial compressive stress were in the range 190.9–233.0 MPa except for one specimen which had a peak axial stress of 47.7 MPa. The elastic parameters were determined at a load corresponding to 50% of the failure load, and it was found that Young's modulus was in the range 69.1–72.2 GPa and that the Poisson ratio was in the range of 0.24–0.27. The specimen with a low compressive strength had a Young's modulus of 63.8 GPa and a Poisson ratio of 0.32.

Sammanfattning

Enaxiella kompressionsprov med belastning upp till brott och strax efter brott har genomförts på 6 stycken vattenmättade cylindriska provobjekt av intakt berg innehållande nätverk med läkta sprickor. Provobjekten har tagits från en borrkärna från borrhål KFM06A i Forsmark. Bergarten hos proverna var medelkornig granit. Proverna har tagits vid en djupnivå som ligger mellan 325–330 m borrhålslängd. De elastiska egenskaperna, representerade av elasticitetsmodulen och Poissons tal, har bestämts ur försöken. Bergmaterialets densitet i vått tillstånd hos proverna mättes upp före de mekaniska proven. Provobjekten fotograferades såväl före som efter de mekaniska proven.

Den uppmätta densiteten hos de vattenmättade proven uppgick till mellan 2 640–2 650 kg/m^3 med ett medelvärde på 2 645 kg/m^3. Toppvärdena för den kompressiva axiella spänningen låg mellan 190,9–233,0 MPa förutom ett prov som hade ett toppvärde på 47,7 MPa. De elastiska parametrarna bestämdes vid en last motsvarande 50 % av högsta värdet på lasten, vilket gav en elasticitetsmodul mellan 69,1–72,2 GPa och Poissons tal mellan 0,24–0,27. Provet som hade en låg kompressionshållfasthet hade en elasticitetsmodul på 68,8 GPa och Poissons tal på 0,32.

Contents

1 Introduction

This document reports performance and results of uniaxial compression tests, with loading just beyond the failure point, on water-saturated drill core specimens sampled from borehole KFM06A at Forsmark, see map in Figure 1-1. The tests were carried out in the material and rock mechanics laboratories at the Department of Building Technology and Mechanics at the Technical Research Institute of Sweden (SP). The activity is part of the site investigation programme at Forsmark managed by SKB (The Swedish Nuclear Fuel and Waste Management Company).

The controlling documents for the activity are listed in Table 1-1. Both Activity Plan and Method Descriptions are SKB's internal controlling documents, whereas the Quality Plan referred to in the table is an SP internal controlling document.

Borehole KFM06A, see Figure 1-1, is a core drilled borehole with a total length of c 1,000 m. The testing has been concentrated to a depth interval between 325–330 m (borehole length) which is located within a zone of a sealed fracture network in medium grained granite (rock type code 101051).

SKB supplied SP with rock cores which arrived at SP in August 2007 and were tested during September 2007. Cylindrical specimens were cut from the cores and selected based on the preliminary core logging with the strategy to investigate the deformation properties of the sealed fracture network in the transition area of the deformation zones in the rock mass. The method description SKB MD 190.001 was followed both for sampling and for the uniaxial compression tests, whereas the density determinations were performed in compliance with method description SKB MD 160.002.

As to the specimen preparation, the end surfaces of the specimens were grinded in order to comply with the required shape tolerances. The specimens were put in water and kept stored in water for a minimum of 7 days, up to density determination and uniaxial testing. This yields a water saturation, which is intended to resemble the in situ moisture condition. The density was determined on each specimen and the uniaxial compression tests were carried out at this moisture condition. The specimens were photographed before and after the mechanical testing.

Table 1-1. Controlling documents for performance of the activity.

Activity Plan	**Number**	**Version**
Tillägg: KFM06A. Bergmekaniska laboratoriebestämningar	AP PF 400-04-121	tillägg
Method Description	**Number**	**Version**
Uniaxial compression test for intact rock	SKB MD 190.001	3.0
Determining density and porosity of intact rock	SKB MD 160.002	2.0
Quality Plan		
SP-QD 13.1		

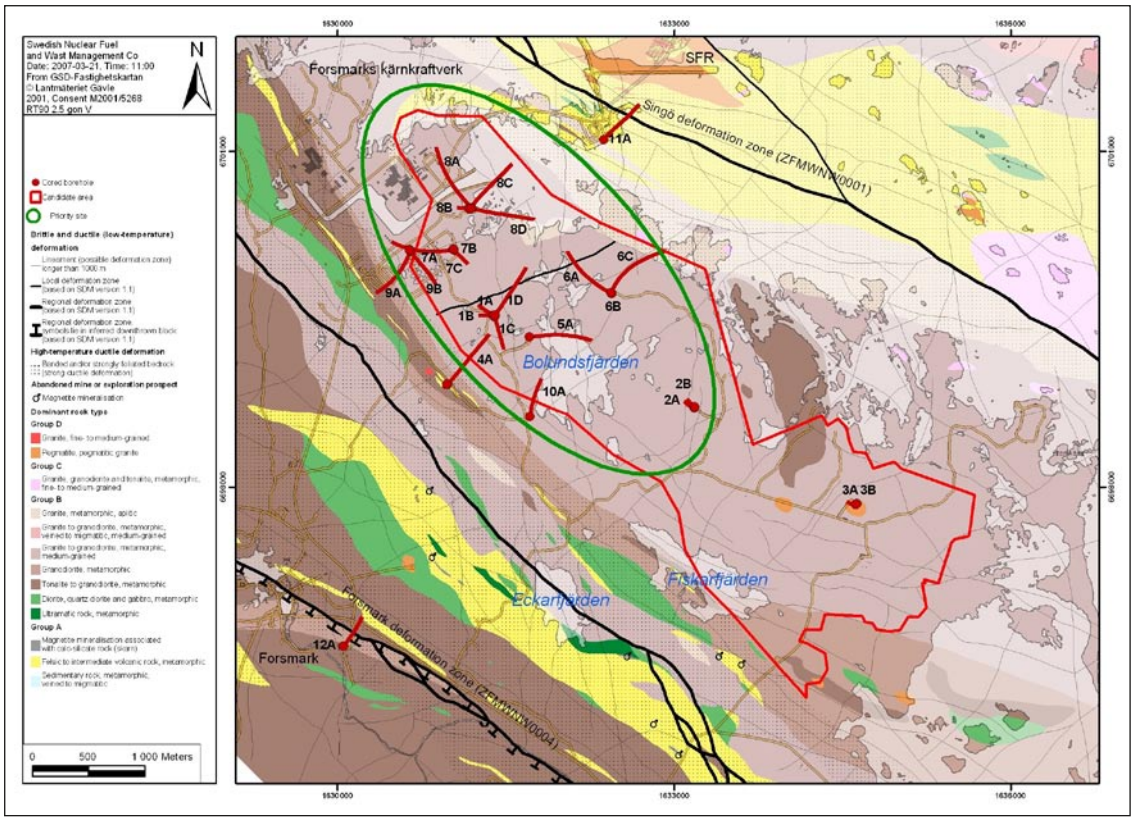

Figure 1-1. *Geological map showing the location of all boreholes drilled up to March 2007 within or close to the Forsmark candidate area. The projection of each borehole on the horizontal plane at top of casing is also shown in the figure.*

The uniaxial compression tests were carried out using radial strain as the feed-back signal as described in the method description SKB MD 190.001 and in the ISRM suggested method /1/. The axial ε_a and radial strain ε_r together with the axial stress σ_a were recorded during the test. The peak value of the axial compressive stress σ_c was determined at each test. Furthermore, two elasticity parameters, Young's modulus E and Poisson ratio v, were deduced from the tangent properties at 50% of the peak load. Diagrams with the volumetric and crack volumetric strain versus axial stress are reported. Results from previous tests on uniaxial compression tests on intact rock core specimens from borehole KFM06A are reported in /2/.

2 Objective

The purpose of the testing is to determine deformation properties of the sealed fracture network in the transition area of the deformation zones in the rock mass. The large scale deformation properties of the rock mass are mainly used in the thermo-mechanical calculations in the site descriptive rock mechanics model contained in the safety assessment programme in conjunction with the site investigations at the candidate area in Forsmark.

The elastic properties, represented by Young's modulus and the Poisson ratio as well as the uni-axial compressive strength were determined on cylindrical specimens of intact rock containing sealed fracture networks sampled from drill cores. Moreover, the specimens had a water content corresponding to the in situ conditions.

3 Equipment

3.1 Specimen preparation and density measurement

A circular saw with a diamond blade was used to cut the specimens to their final lengths. The surfaces were then grinded after cutting in a grinding machine in order to achieve a high-quality surface for the axial loading that complies with the required tolerances. The measurements of the specimen dimensions were made with a sliding calliper. Furthermore, the tolerances were checked by means of a dial indicator and a stone face plate. The specimen preparation is carried out in accordance with ASTM 4543-01 /3/.

The specimens and the water were weighed using a scale for weight measurements. A thermometer was used for the water temperature measurement. The calculated wet density was determined with an uncertainty of ± 4 kg/m^3.

3.2 Mechanical testing

The mechanical tests were carried out in a servo controlled testing machine specially designed for rock tests, see Figure 3-1. The system consists of a load frame, a hydraulic pump unit, a controller unit and various sensors. The communication with the controller unit is accomplished by means of special testing software run on a PC connected to the controller. The load frame is characterized by a high stiffness and is supplied with a fast responding actuator, cf the ISRM suggested method /1/.

Figure 3-1. *Rock testing system. From left: Digital controller unit, pressure cabinet (used for triaxial tests) and load frame. The PC with the test software (not shown in the picture) is placed on the left hand side of the controller unit.*

The stiffness of the various components of the loading chain in the load frame has been optimized in order to obtain a high total stiffness. This includes the load frame, load cell, load platens and piston, as well as having a minimum amount of hydraulic oil in the cylinder. Furthermore, the sensors, the controller and the servo valve are rapidly responding components. The axial load is determined using a load cell, which has a maximum capacity of 1.5 MN. The uncertainty of the load measurement is less than 1%.

The axial and circumferential (radial) deformations of the rock specimens were measured. The rock deformation measurement systems are based on miniature LVDTs with a measurement range of ± 2.5 mm. The relative error for the LVDTs is less than 0.6% within a 1 mm range for the axial deformation measurements and less than 1.3% within a 3 mm range for the circumferential deformation measurement. The LVDTs have been calibrated by means of a micrometer.

Two independent systems were used for the axial deformation measurement in order to obtain two comparative results. The first system (S1), see Figure 3-2, comprises two aluminium rings attached on the specimen, placed at ¼ and ¾ of the specimen height. Two LVDTs mounted on the rings are used to measure the distance change between the rings on opposite sides of the specimen. As to the attachment, two rubber bands made of a thin rubber hose with 0.5 mm thickness are first mounted on the specimen right under where the two rings are to be positioned. The rings are supplied with three adjustable spring-loaded screws, each with a rounded tip pointing on the specimen with 120 degrees division. The screw tips are thus pressing on the rubber band, when the rings are mounted. The second system (S2), see Figure 3-3, consists of two aluminium plates clamped around the circular loading platens of steel on top and on bottom of the specimen. Two LVDTs, mounted on the plates, measure the distance change between these plates at opposite sides of the specimen at corresponding positions as for the first measurement system (S1).

The radial deformation was obtained by using a chain mounted around the specimen at mid-height; see Figures 3-2 and 3-3. The change of the chain-opening gap was measured by means of one LVDT and the circumferential, and thereby also the radial deformation could be obtained. See Appendix A.

The specimens were photographed with a 4.0 Mega pixel digital camera at highest resolution and the photos were stored in a jpeg-format.

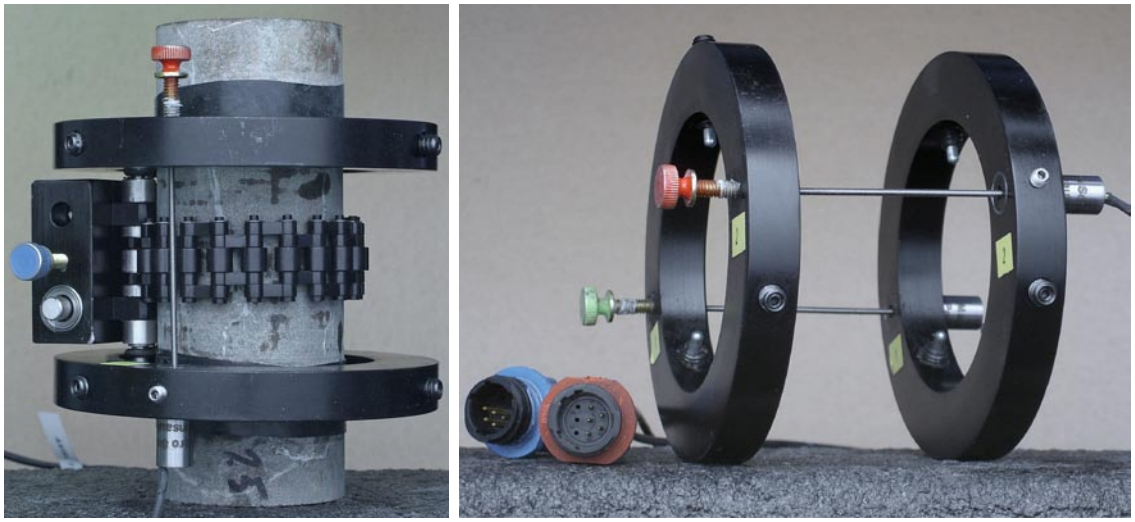

Figure 3-2. *Left: Specimen with two rubber bands. Devices for local axial and circumferential deformation measurements attached on the specimen. Right: Rings and LVDTs for local axial deformation measurement.*

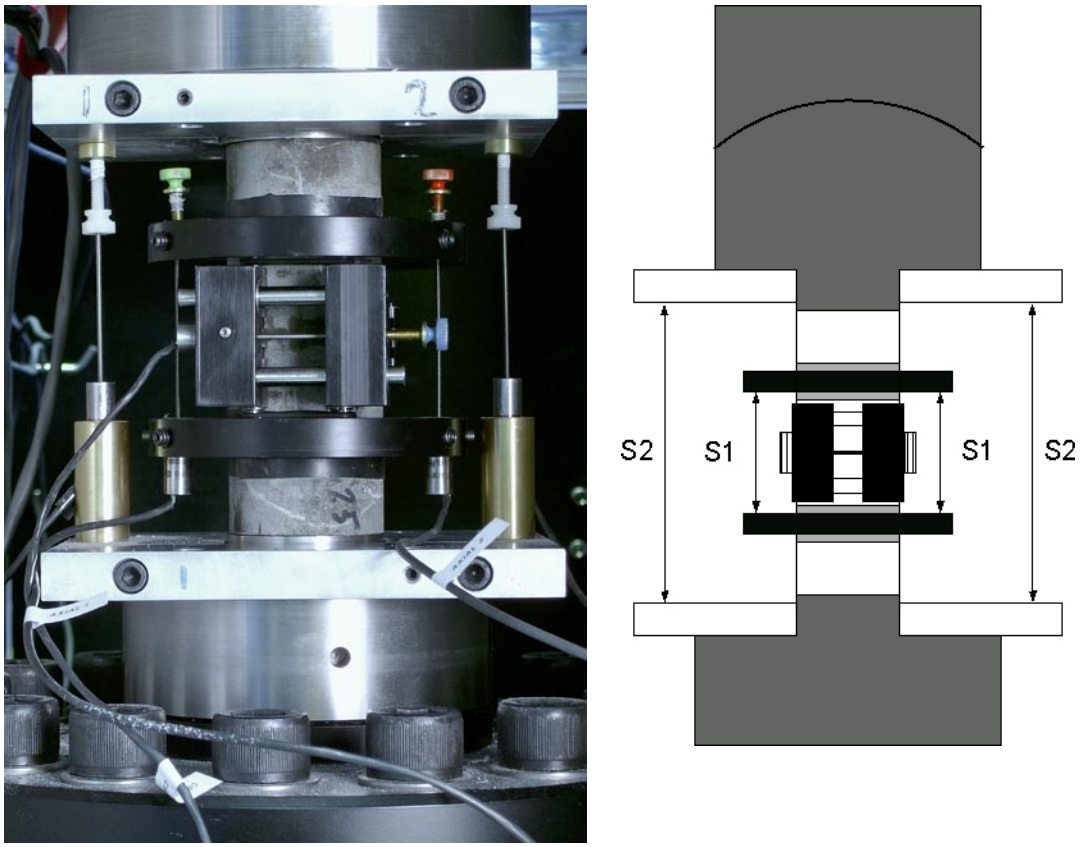

Figure 3-3. *Left: Specimen inserted between the loading platens. The two separate axial deformation measurement devices can be seen: system (S1) that measures the local axial deformation (rings), and system (S2) that measures the deformation between the aluminium plates (total deformation). Right: Principal sketch showing the two systems used for the axial deformation measurements.*

4 Execution

The water saturation and determination of the density of the wet specimens were made in accordance with the method description SKB MD 160.002 (SKB internal controlling document). This includes determination of density in accordance to ISRM /4/ and water saturation by SS EN 13755 /5/. The uniaxial compression tests were carried out in compliance with the method description SKB MD 190.001 (SKB internal controlling document). The test method is based on ISRM suggested method /1/.

4.1 Description of the specimens

The rock type characterisation was made according to Stråhle /6/ using the SKB mapping system (Boremap). The identification marks, upper and lower sampling depth (secup and seclow) and the rock type are shown in Table 4-1.

4.2 Specimen preparation and density measurement

The temperature of the water was 17.5°C, which equals to a water density of 998.7 kg/m^3, when the determination of the wet density of the rock specimens was carried out. Further, the specimens had been stored during 8 days in water when the density was determined.

An overview of the activities during the specimen preparation is shown in the step-by step description in Table 4-2.

4.3 Mechanical testing

The specimens had been stored 22 days in water when the uniaxial compression tests were carried out. The functionality of the testing system was checked before starting the tests. A check-list was filled in successively during the work in order to confirm that the different specified steps had been carried out. Moreover, comments were made upon observations made during the mechanical testing that are relevant for interpretation of the results. The check-list form is an SP internal quality document.

An overview of the activities during the mechanical testing is shown in the step-by step description in Table 4-3.

Table 4-1. Specimen identification, sampling level (borehole length) and rock type for all specimens (based on the Boremap).

Identification	Adj secup (m)	Adj seclow (m)	Rock type/occurrence
KFM06A-113-21	325.481	325.629	Medium grained granite (101051), sealed fracture network
KFM06A-113-22	327.786	327.939	Medium grained granite (101051), sealed fracture network
KFM06A-113-23	328.044	328.197	Medium grained granite (101051), sealed fracture network
KFM06A-113-24	328.346	328.499	Medium grained granite (101051), sealed fracture network
KFM06A-113-25	328.676	328.828	Medium grained granite (101051), sealed fracture network
KFM06A-113-26	330.691	330.844	Medium grained granite (101051), sealed fracture network

Table 4-2. Activities during the specimen preparation.

Step	Activity
1	The drill cores were marked where the specimens are to be taken.
2	The specimens were cut to the specified length according to markings and the cutting surfaces were grinded.
3	The tolerances were checked: parallel and perpendicular end surfaces, smooth and straight circumferential surface.
4	The diameter and height were measured three times each. The respective mean value determines the dimensions that are reported.
5	The specimens were then water saturated according to the method described in SKB MD 160.002 and were stored for minimum 7 days in water, whereupon the wet density was determined.

Table 4-3. Activities during the mechanical testing.

Step	Activity
1	Digital photos were taken on each specimen before the mechanical testing.
2	Devices for measuring axial and circumferential deformations were attached to the specimen.
3	The specimen was put in place and centred between the frame loading platens.
4	The core on each LVDT was adjusted by means of a set screw to the right initial position. This was done so that the optimal range of the LVDTs can be used for the deformation measurement.
5	The frame piston was brought down into contact with the specimen with a force corresponding to 1.0 MPa axial stress.
6	A load cycle with loading up to 5 MPa and unloading to 1.0 MPa was conducted in order to settle possible contact gaps in the spherical seat in the piston and between the rock specimen and the loading platens.
7	The centring was checked again.
8	The deformation measurement channels were zeroed in the test software.
9	The loading was started and the loading rate was set to a radial strain rate of –0.025%/min.
10	The test was manually stopped shortly after the peak load had been reached.
11	Digital photos were taken on each specimen after the mechanical testing.

4.4 Data handling

The test results were exported as text files from the test software and stored in a file server on the SP computer network after each completed test. The main data processing, in which the elastic moduli were computed and the peak stress was determined, has been carried out using the program MATLAB /7/. Moreover, MATLAB was used to produce the diagrams shown in Section 5.1 and in Appendix B. The summary of results in Section 5.2 with tables containing mean value and standard deviation of the different parameters and diagrams were provided using MS Excel. MS Excel was also used for reporting data to the Sicada database.

4.5 Analyses and interpretation

As to the definition of the different results parameters we begin with the axial stress σ_a, which is defined as

$$\sigma_a = \frac{F_a}{A}$$

where F_a is the axial force acting on the specimen, and A is the specimen cross section area. The peak value of the axial stress during a test is representing the uniaxial compressive strength σ_c in the results presentation.

The average value of the two axial displacement measurements on opposite sides of the specimen is used for the axial strain calculation, cf Figure 3-3. In the first measurement system (S1), the recorded deformation represents a local axial deformation δ_{local} between the points at ¼ and ¾ height. A local axial strain is defined as

$$\varepsilon_{a,local} = \delta_{local}/L_{local}$$

where L_{local} is the distance between the rings before loading.

In the second measurement system (S2), the recorded displacement corresponds to a total deformation that, in addition to total rock deformation, also contains the local deformations that occur in the contact between the rock and the loading platens, and further it also contains the deformation of the steel loading platens at each side of the specimen ends. The average value of the two total deformation measurements on opposite sides of the specimen is defined as the total deformation δ_{total}. An axial strain based on the total of the deformation is defined as

$$\varepsilon_{a,total} = \delta_{total}/L_{total}$$

where L_{total} is the height of the rock specimen.

The radial deformation is measured by means of a chain mounted around the specimen at mid-height, cf Figures 3-2 and 3-3. The change of chain opening gap is measured by means of one LVDT. This measurement is used to compute the radial strain ε_r, see Appendix A. Moreover, the volumetric strain ε_{vol} is defined as

$$\varepsilon_{vol} = \varepsilon_a + 2\varepsilon_r$$

The stresses and the strains are defined as positive in compressive loading and deformation. The elasticity parameters are defined by the tangent Young's modulus E and tangent Poisson ratio ν as

$$E = \frac{\sigma_a(0.60\sigma_c) - \sigma_a(0.40\sigma_c)}{\varepsilon_a(0.60\sigma_c) - \varepsilon_a(0.40\sigma_c)}$$

$$\nu = -\frac{\varepsilon_r(0.60\sigma_c) - \varepsilon_r(0.40\sigma_c)}{\varepsilon_a(0.60\sigma_c) - \varepsilon_a(0.40\sigma_c)}$$

The tangents were evaluated with values corresponding to an axial load between 40% and 60% of the axial peak stress σ_c.

Two important observations can be made from the results:

(i) The results based on the total axial deformation measurement (S2) display a lower axial stiffness, i.e. a lower value on Young's modulus, than in the case when the results are based on the local axial deformation measurement (S1). This is due to the additional deformations from the contact interface between the rock specimen and the steel loading platens and also due to the deformation of the loading platens themselves.

(ii) It can be seen that the response differs qualitatively between the results obtained with the local axial deformation measurement system (S1) and the system that measures total axial deformation (S2). In some cases the post-peak response obtained with the local deformation measurement system seems not to be physically correct. This can be due to a number of reasons, e.g. that a crack caused a localized deformation, see Figure 4-1. Another explanation could be that the rings attached to the specimens have slightly slipped or moved, for example if a crack was formed nearby one of the attachment points.

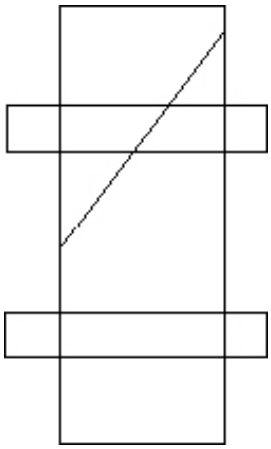

Figure 4-1. *Example of cracking that may cause results that are difficult to interpret with a local deformation measurement.*

It is reasonable to assume that results based on the local axial deformation measurement (S1) are fairly accurate up to the formation of the first macro-cracks or up to the peak load, but not thereafter. However, the results obtained with the total axial deformation measurement (S2) seem to be qualitatively correct after failure. We will therefore report the results based on the total axial deformation measurement, but carry out a correction of those results as described below in order to obtain overall good results.

The total axial deformation δ_{total} measured by (S2) is a summation of several deformations

$$\delta_{total} = \delta_{rock} + \delta_{system} \quad (1)$$

where

$$\delta_{system} = \delta_{interface} + \delta_{loading\ platens}$$

and δ_{rock} is the axial deformation of the whole rock specimen. Assume that the system deformation is proportional to the applied axial force F_a in the loading chain, i.e.

$$\delta_{system} = F_a/K_{system} \quad (2)$$

where K_{system} is the axial stiffness in the system (containing the interface between the rock and loading platens and the deformation of the loading platens). Combining (1) and (2) leads to

$$\delta_{rock} = \delta_{total} - F_a/K_{system} \quad (3)$$

where an expression of the axial deformation in the whole specimen is obtained. This can be viewed as a correction of the measurements made by system (S2). By using δ_{rock} to represent the axial deformation of the specimen that is based on a correction of the results of the total axial deformation will yield good results both in the loading range up to failure and at loading after failure. However, it is noticed that K_{system} is not known and has to be determined.

It was previously suggested that the local axial deformation measurement (S1) represents the real rock deformation well up to the load where the macro-cracks form. Further, it is fair to assume that the axial deformation is homogenous at this part of the loading. Hence, we get

$$\delta_{rock} = \delta_{local} \cdot L_{total}/L_{local} \quad (4)$$

This yields representative values of the total rock deformation for the first part of the loading up to the point where macro-cracking is taking place. It is now possible to determine δ_{system} up to the threshold of macro-cracking by combining (1) and (4) which yields

$$\delta_{system} = \delta_{total} - \delta_{local} \cdot L_{total}/L_{local} \quad (5)$$

Finally, we need to compute K_{system}. By rewriting (2) we get

$$K_{system} = \frac{F_a}{\delta_{system}}$$

We will compute the system stiffness based on the results between 40% and 60% of the axial peak stress σ_c. This means that the Young's modulus and the Poisson ratio will take the same values both when the data from the local axial deformation measurement (S1) and when the data from corrected total axial deformation are used. Thus, we have

$$K_{system} = \frac{F_a(0.60\sigma_c) - F_a(0.40\sigma_c)}{\delta_{system}(0.60\sigma_c) - \delta_{system}(0.40\sigma_c)} \quad (6)$$

The results based on the correction according to (3) and (6) are presented in Section 5.1, whereas the original measured unprocessed data are reported in Appendix B.

Results on volumetric strain and crack volume strain are reported. By subtracting the elastic volumetric strain ε_{vol}^{e} from the total volumetric strain, a volumetric strain corresponding to the crack volume ε_{vol}^{cr} is obtained. This has been denoted calculated crack volumetric strain in the literature, cf /8, 9/. We thus have

$$\varepsilon_{vol}^{cr} = \varepsilon_{vol} - \varepsilon_{vol}^{e}$$

Assuming linear elasticity leads to

$$\varepsilon_{vol}^{cr} = \varepsilon_{vol} - \frac{1-2\nu}{E}\sigma_a$$

where $\sigma_r = 0$ was used. The axial stresses on which the onset of an increased crack volume strain and total volumetric strain during uniaxial compression of intact rock core specimens without sealed joints occur, have commonly been related to the crack initiation stress σ_i and the crack damage stress σ_d respectively, cf /8, 9/. The interpretation of the volumetric strains results versus axial stress is, however, unclear when the rock contains sealed joints.

4.6 Nonconformities

The testing was conducted according to the method description with some deviations. The testing was stopped prematurely right after the peak load was obtained and thereby not registering the complete stress-strain response according to the the ISRM-standard /1/. Moreover, the circumferential strains have been determined within a relative error of 1.5%, which is larger than what is specified in the ISRM-standard /1/. Further, double systems for measuring the axial deformation have been used, which is beyond the specifications in the method description. This was conducted as development of the test method specially aimed for high-strength brittle rock.

Specimen KFM06A-113-26 displayed a significantly lower strength than the other tested specimens and it was decided to complement the results by testing the spare specimen KFM06A-113-24 as well. Besides this, the activity plan was followed with no departures.

5 Results

The results of the individual specimens are presented in Section 5.1 and a summary of the results is given in Section 5.2. The reported parameters are based both on unprocessed raw data obtained from the testing and processed data and were reported to the Sicada database, where they are traceable by the activity plan number. These data together with the digital photographs of the individual specimens were handed over to SKB. The handling of the results follows SDP-508 (SKB internal controlling document) in general.

5.1 Results for each individual specimen

The cracking is shown in photos of the specimens, and comments on observations made during the testing are reported. The elasticity parameters have been evaluated by using the results from the local axial deformation measurements. The data from the adjusted total axial deformation measurements, cf Section 4.4, are shown in this section. Red rings are superposed on the graphs indicating every five minutes of the progress of testing.

Diagrams showing the data from both the local and the total axial deformation measurements, system (S1) and (S2) in Figure 3-3, and the computed individual values of K_{system} used at the data corrections are shown in Appendix B. Diagrams displaying actual radial strain rates versus the test time are also presented in Appendix B. The results for the individual specimens are as follows:

Specimen ID: KFM06A-113-21

Before mechanical test **After mechanical test**

Diameter (mm)	Height (mm)	Density (kg/m^3)
50.6	128.7	2,650

Comments: A small chip has been spalled out slightly above the mid height of the specimen.

Specimen ID: KFM06A-113-21

Youngs Modulus (E):	69.1	[GPa]
Poisson Ratio (ν):	0.247	[-]
Axial peak stress (σ_c):	220.9	[MPa]

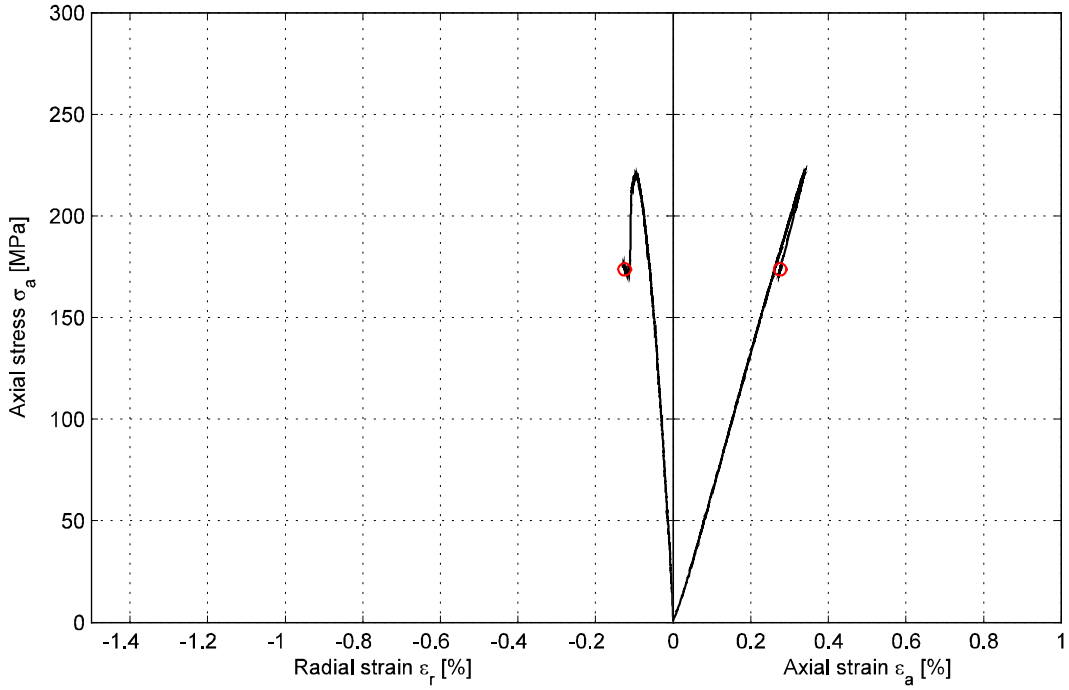

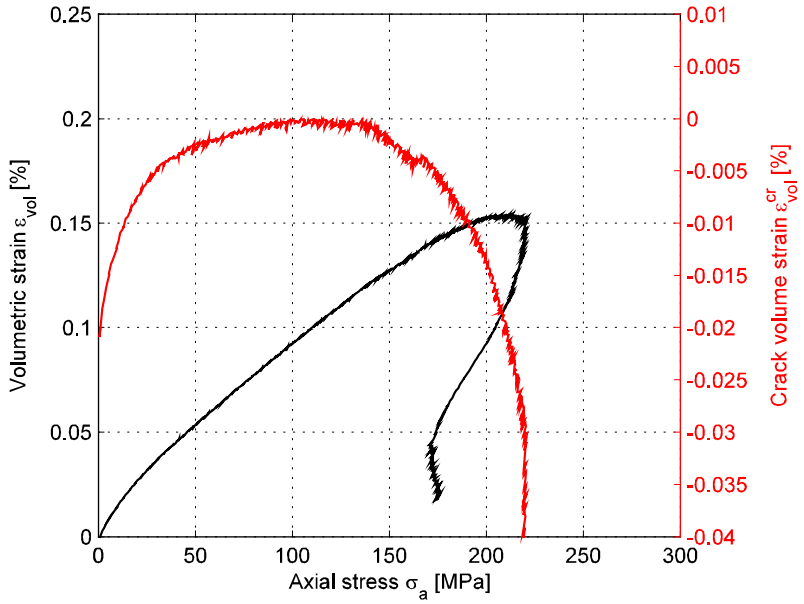

Specimen ID: KFM06A-113-22

Before mechanical test **After mechanical test**

Diameter (mm)	Height (mm)	Density (kg/m^3)
50.6	128.7	2,650

Comments: A small chip has been spalled out at two locations approximately at the mid-height of the specimen along an existing selaed joint.

Specimen ID: KFM06A-113-22

Youngs Modulus (E):	70.9	[GPa]
Poisson Ratio (ν):	0.24	[-]
Axial peak stress (σ_c):	190.9	[MPa]

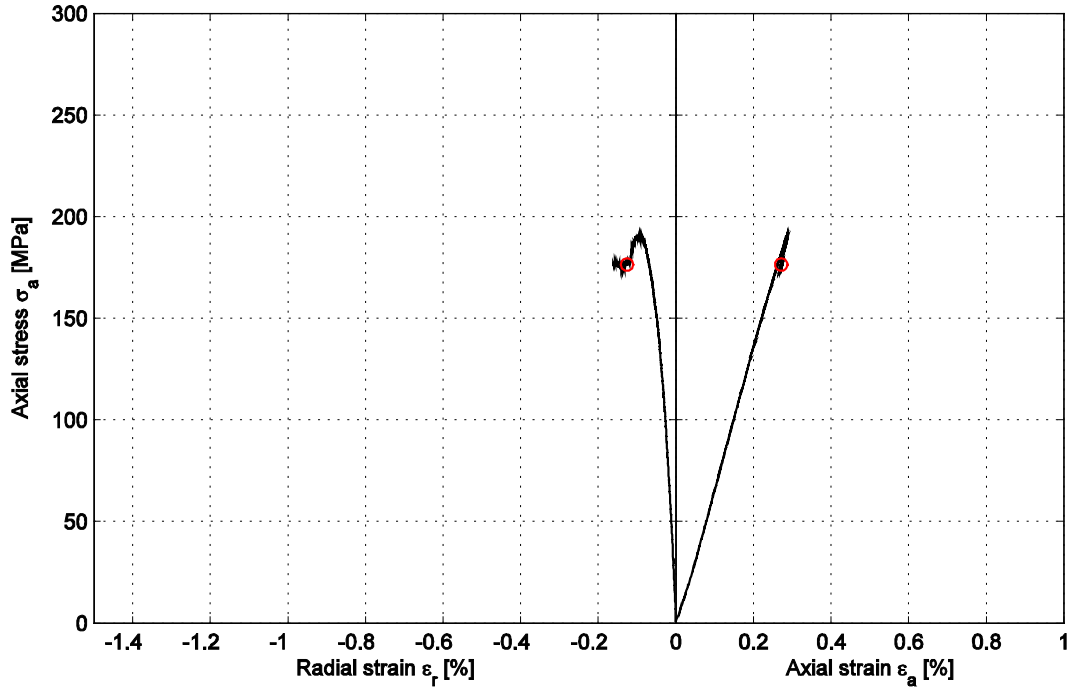

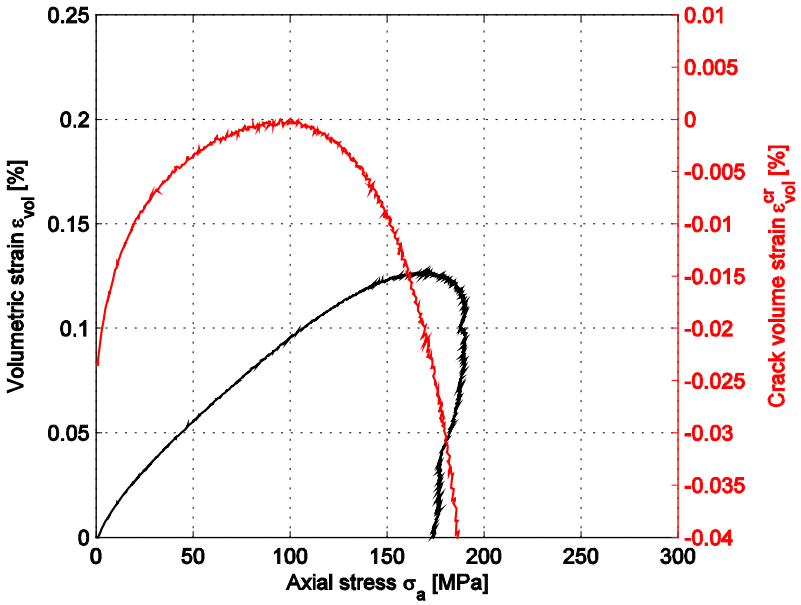

Specimen ID: KFM06A-113-23

Before mechanical test **After mechanical test**

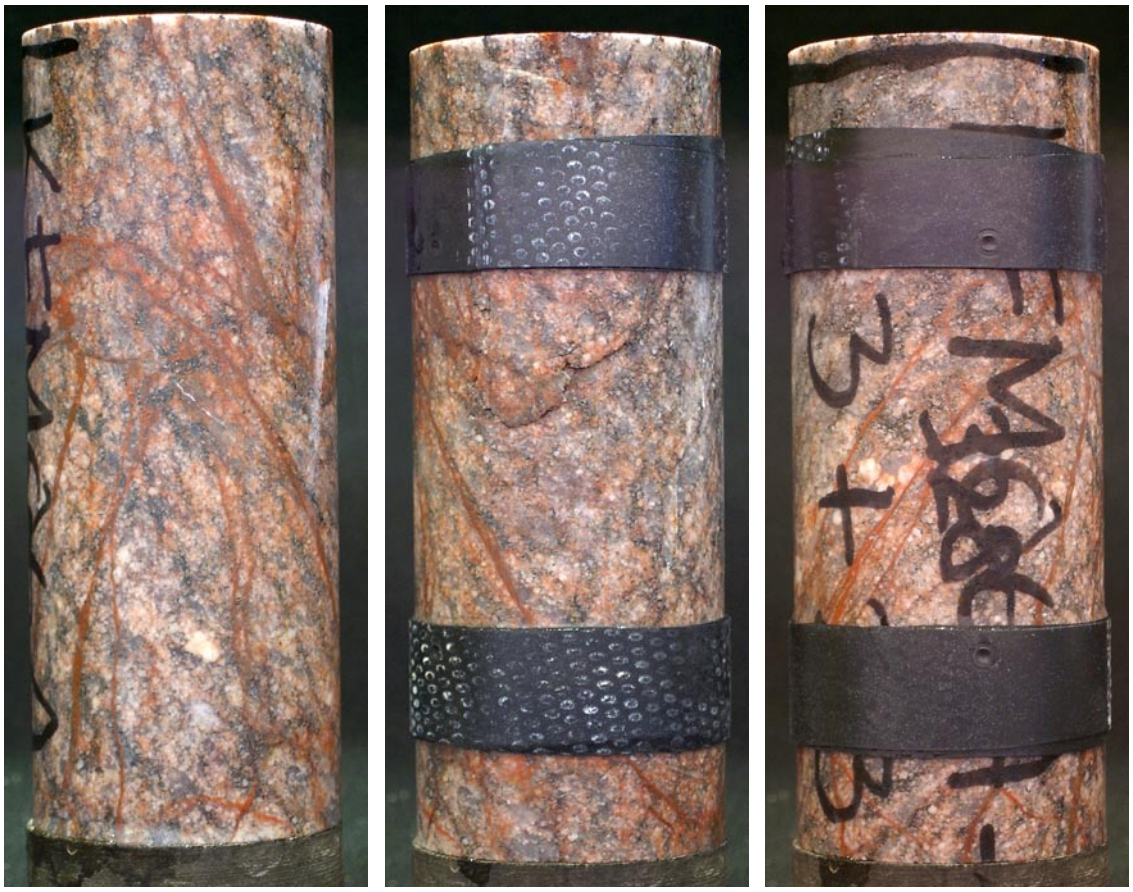

Diameter (mm)	Height (mm)	Density (kg/m^3)
50.6	128.6	2,650

Comments: Spalling is observed on one side at the upper half of the specimen, which seems to follow an existing sealed joint. A second fracture following the rock texture has started to develop.

Specimen ID: KFM06A-113-23

Youngs Modulus (E):	71.5	[GPa]
Poisson Ratio (ν):	0.246	[-]
Axial peak stress (σ_c):	223.4	[MPa]

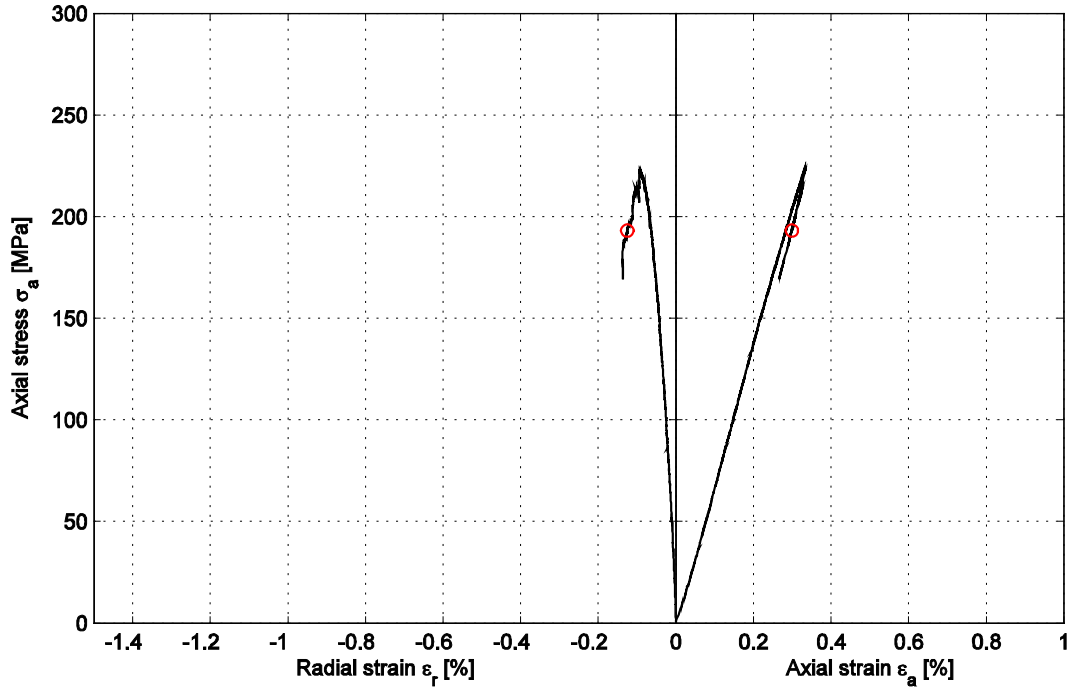

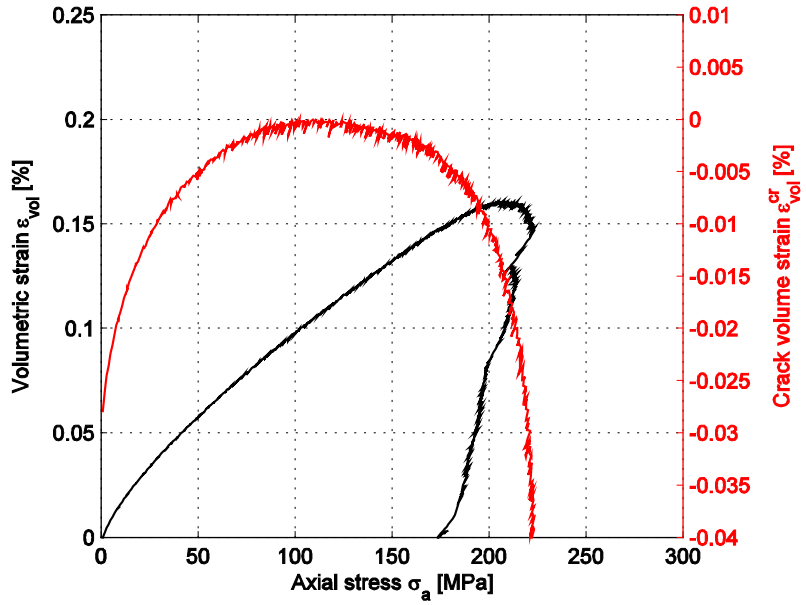

Specimen ID: KFM06A-113-24

Before mechanical test **After mechanical test**

Diameter (mm)	Height (mm)	Density (kg/m^3)
50.6	128.7	2,640

Comments: Spalling has started to develop at mid-height of the specimen.

Specimen ID: KFM06A-113-24

Youngs Modulus (E):	72.2	[GPa]
Poisson Ratio (ν):	0.245	[-]
Axial peak stress (σ_c):	231.7	[MPa]

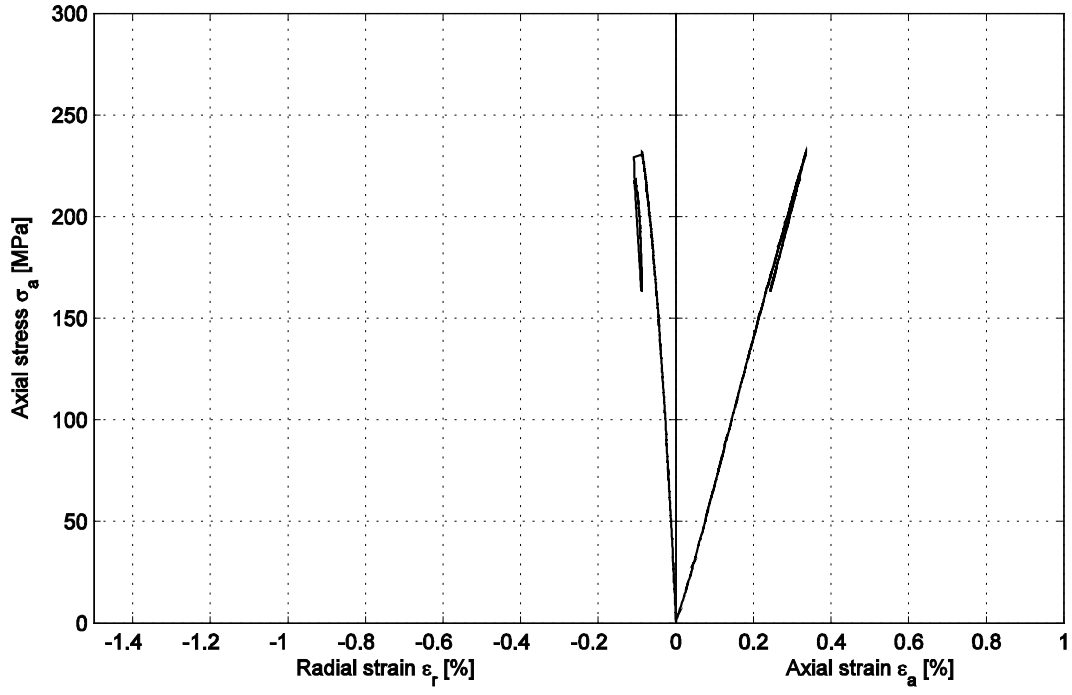

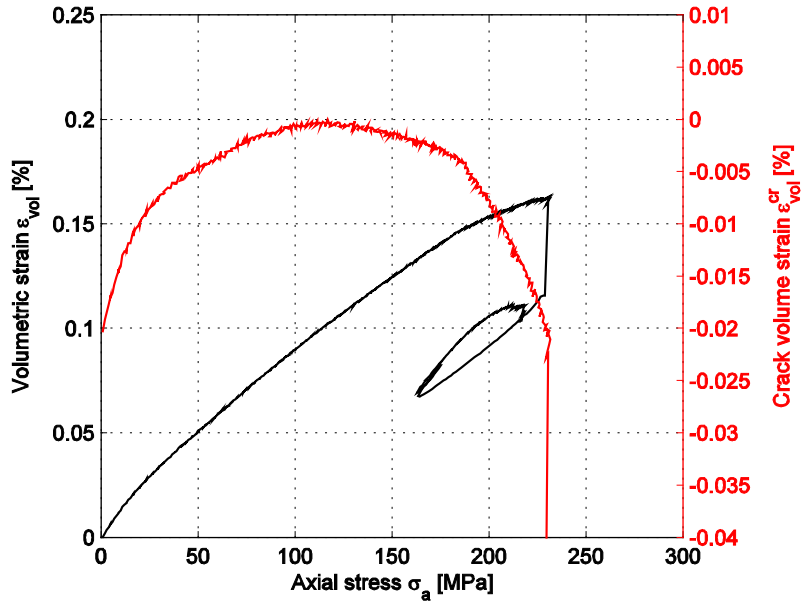

Specimen ID: KFM06A-113-25

Before mechanical test **After mechanical test**

Diameter (mm)	Height (mm)	Density (kg/m^3)
50.6	128.6	2,640

Comments: Spalling has started to develop at mid-height of the specimen in an area with a mineral inclusion.

Specimen ID: KFM06A-113-25

Youngs Modulus (E):	71.2	[GPa]
Poisson Ratio (ν):	0.269	[-]
Axial peak stress (σ_c):	233	[MPa]

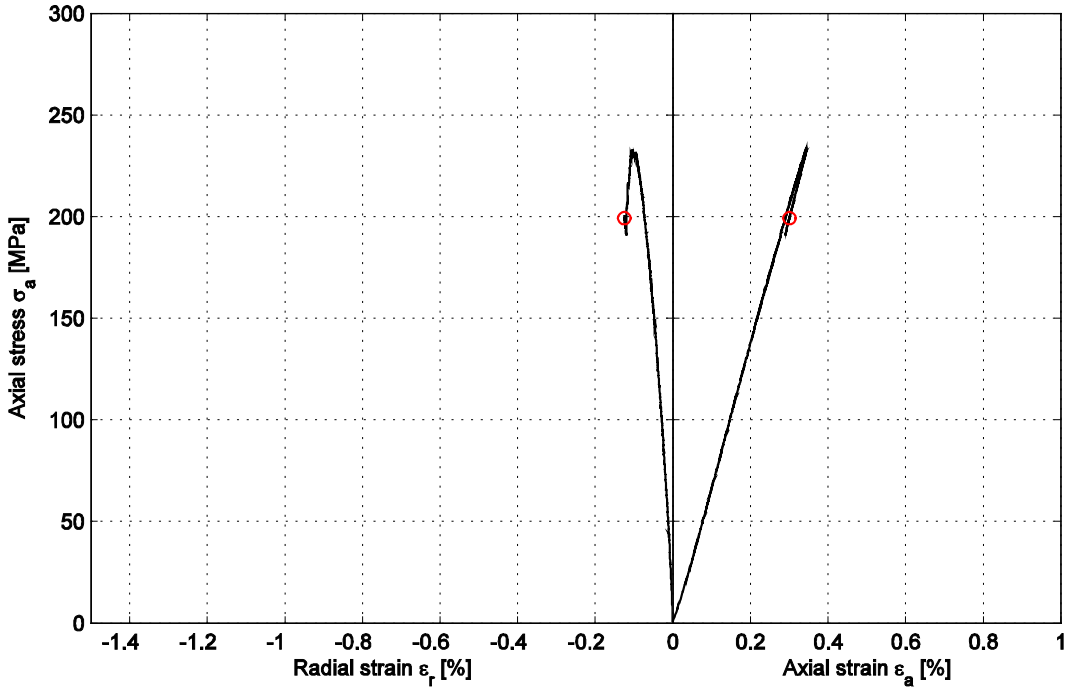

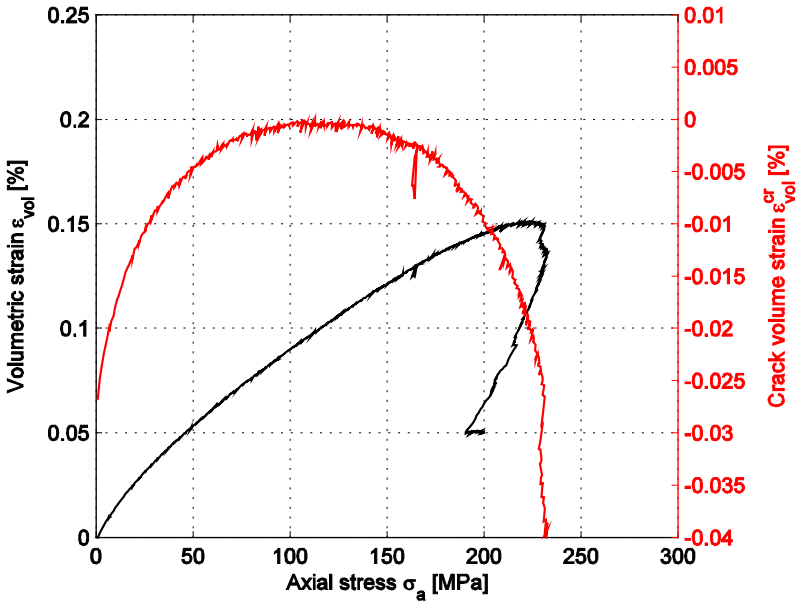

Specimen ID: KFM06A-113-26

Before mechanical test **After mechanical test**

Diameter (mm)	Height (mm)	Density (kg/m^3)
50.7	128.7	2,640

Comments: A vertical fracture has developed along the specimen.

Specimen ID: KFM06A-113-26

Youngs Modulus (E):	63.8	[GPa]
Poisson Ratio (ν):	0.319	[-]
Axial peak stress (σ_c):	47.7	[MPa]

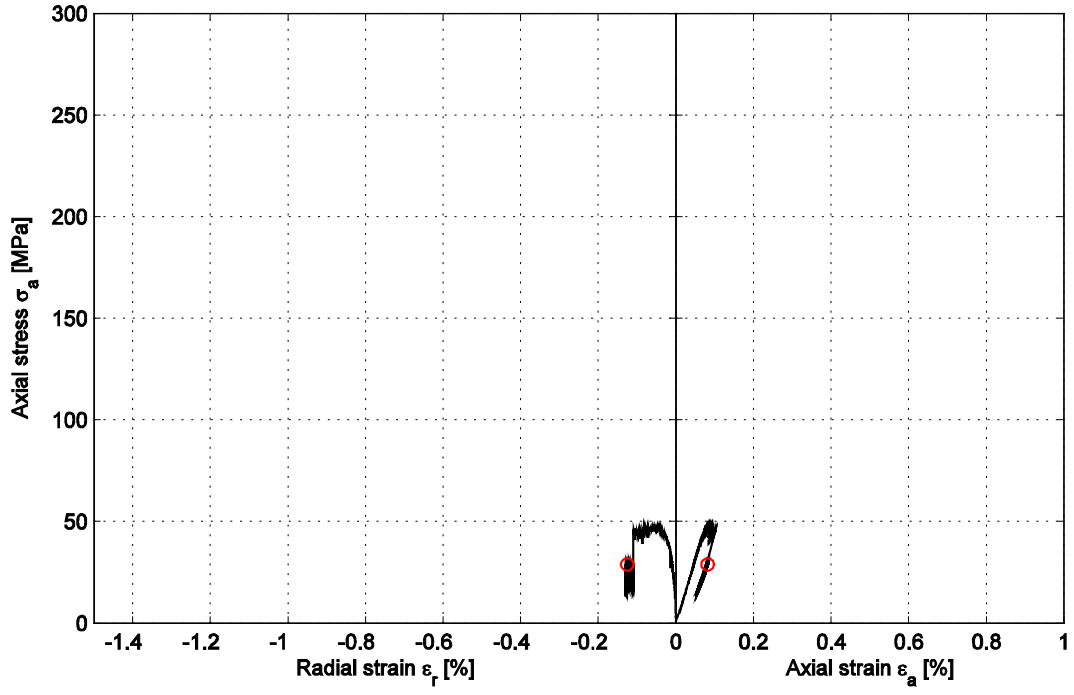

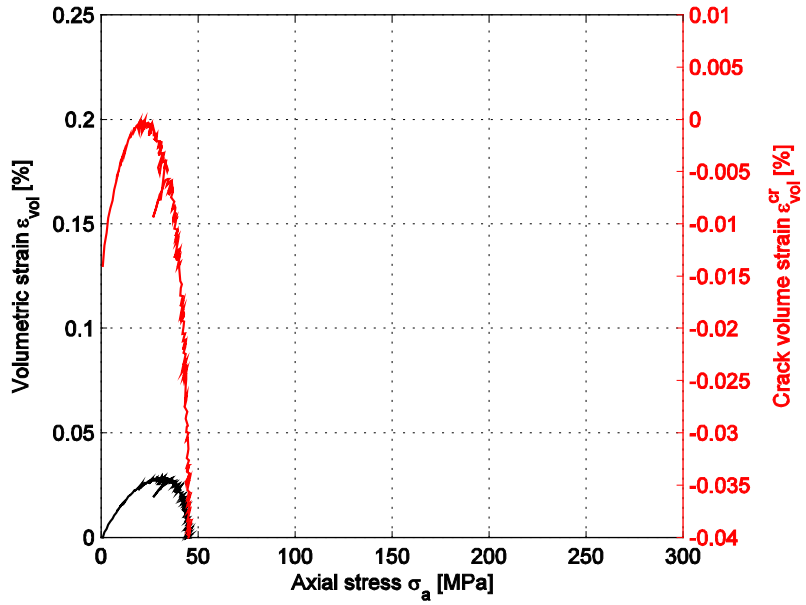

5.2 Results for the entire test series

A summary of the test results is shown in Table 5-1. The density, the uniaxial compressive strength, the tangent Young's modulus and the tangent Poisson ratio versus sampling level (borehole length) are shown in Figures 5-1 to 5-4.

Table 5-1. Summary of results.

Identification	Density (kg/m^3)	Compressive strength (MPa)	Young's modulus (GPa)	Poisson ratio (–)	K_{system} (GN/m)
KFM06A-113-21	2,650	220.9	69.1	0.25	34.6
KFM06A-113-22	2,650	190.9	70.9	0.24	25.2
KFM06A-113-23	2,650	223.4	71.5	0.25	22.0
KFM06A-113-24	2,640	231.7	72.2	0.24	19.7
KFM06A-113-25	2,640	233.0	71.2	0.27	25.1
KFM06A-113-26	2,640	47.7	63.8	0.32	6.0

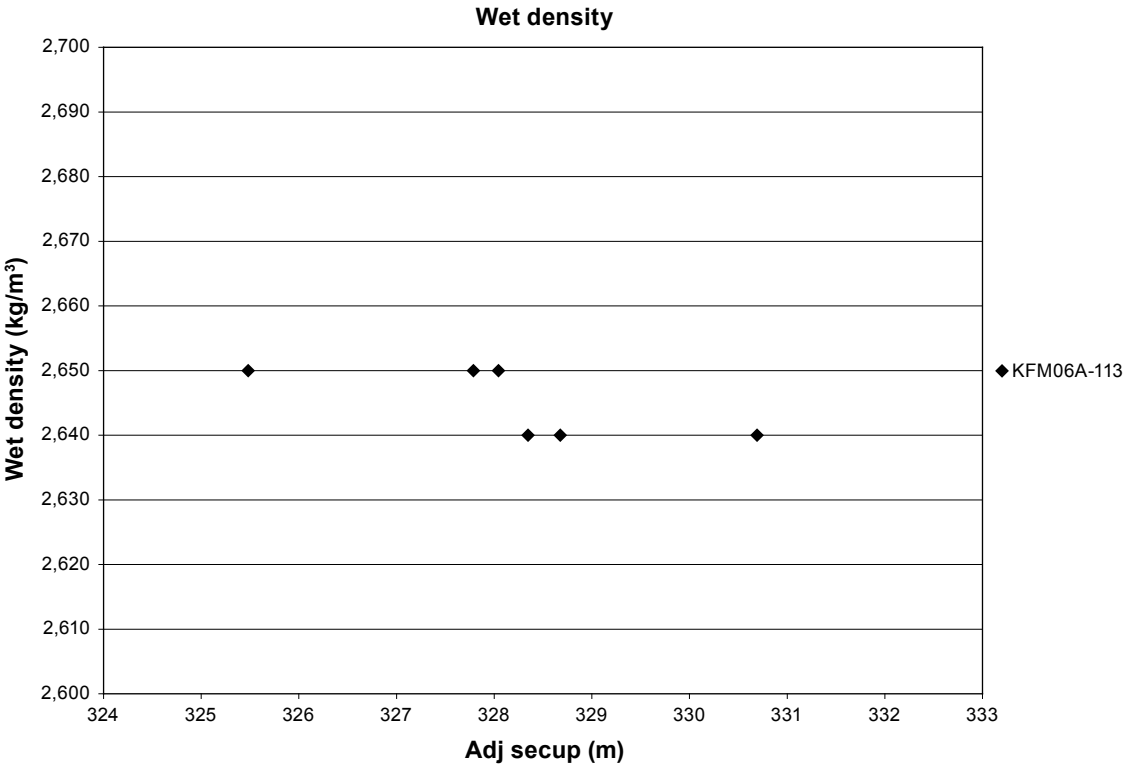

Figure 5-1. *Density versus sampling level (borehole length).*

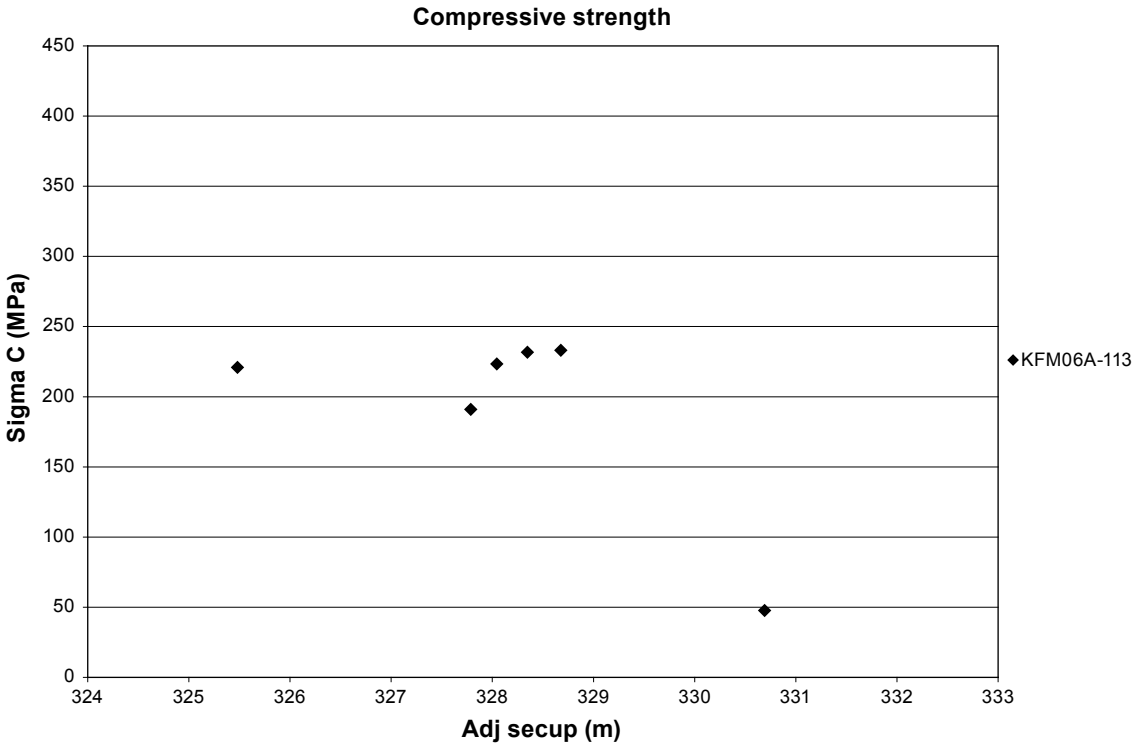

Figure 5-2. *Uniaxial compressive strength versus sampling level (borehole length).*

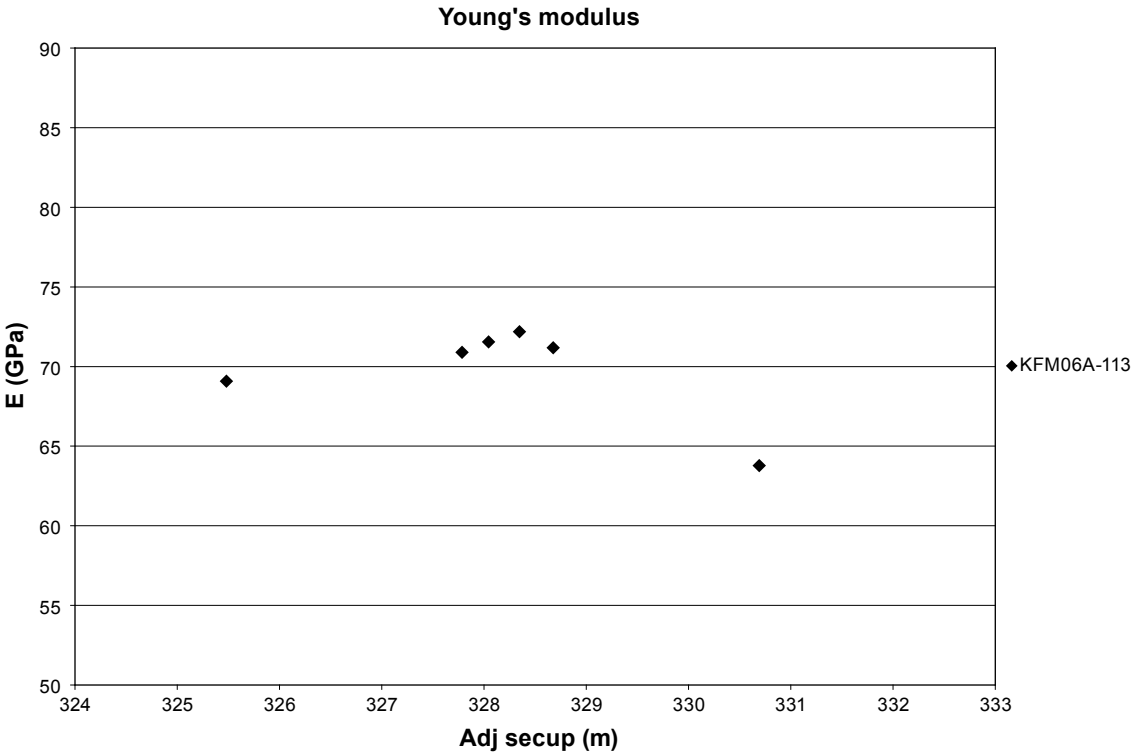

Figure 5-3. *Tangent Young's modulus versus sampling level (borehole length).*

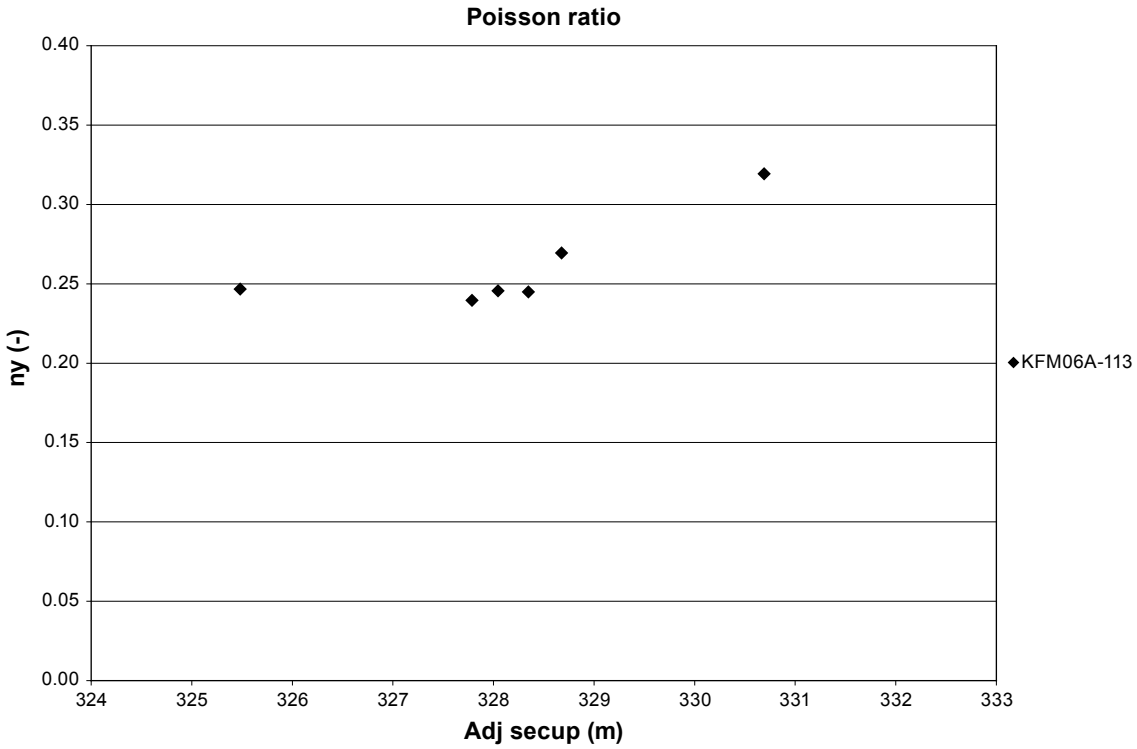

Figure 5-4. *Tangent Poisson ratio versus sampling level (borehole length).*

References

/1/ **ISRM, 1999.** Draft ISRM suggested method for the complete stress-strain curve for intact rock in uniaxial compression. Int. J. Rock. Mech. Min. Sci. 36(3), pp. 279–289.

/2/ **Jacobsson L, 2005.** Forsmark site investigation. Borehole KFM06A. Uniaxial compression test of intact rock. SKB P-05-120, Svensk kärnbränslehantering AB.

/3/ **ASTM 4543-01, 2001.** Standard practice for preparing rock core specimens and determining dimensional and shape tolerance.

/4/ **ISRM, 1979.** Suggested Method for Determining Water Content, Porosity, Density, Absorption and Related Properties and Swelling and Slake-durability Index Properties. Int. J. Rock. Mech. Min. Sci. & Geomech. Abstr. 16(2), pp. 141–156.

/5/ **SS-EN 13755.** Natural stone test methods – Determination of water absorption at atmospheric pressure.

/6/ **Stråhle A, 2001.** Definition och beskrivning av parametrar för geologisk, geofysisk och bergmekanisk kartering av berg. SKB R-01-19, Svensk kärnbränslehantering AB. In Swedish.

/7/ **MATLAB, 2002.** The Language of Technical computing. Version 6.5. MathWorks Inc.

/8/ **Martin C D, Chandler N A, 1994.** The progressive fracture of Lac du Bonnet granite. Int. J. Rock. Mech. Min. Sci. & Geomech. Abstr. 31(6), pp. 643–659.

/9/ **Eberhardt E, Stead D, Stimpson B, Read R S, 1998.** Identifying crack initiation and propagation thresholds in brittle rock. Can. Geotech. J. 35, pp. 222–233.

Appendix A

The following equations describe the calculation of radial strains when using a circumferential deformation device, see Figure A-1.

$$\varepsilon_r = \frac{\Delta C}{C_i}$$

where

$C_i = 2\,\pi\,R_i$ = initial specimen circumference

$\Delta\,C$ = change in specimen circumference = $\dfrac{\pi \cdot \Delta X}{\sin\left(\dfrac{\theta_i}{2}\right) + \left(\pi - \dfrac{\theta_i}{2}\right)\cos\left(\dfrac{\theta_i}{2}\right)}$

and

$\Delta\,X$ = change in LVDT reading = $X_i - X_f$

(X_i = initial chain gap; X_f = current chain gap)

θ_i = initial chord angle = $2\,\pi - \dfrac{L_c}{R_i + r}$

L_c = chain length (measured from center of one end roller to center of the other end roller)

r = roller radius

R_i = initial specimen radius

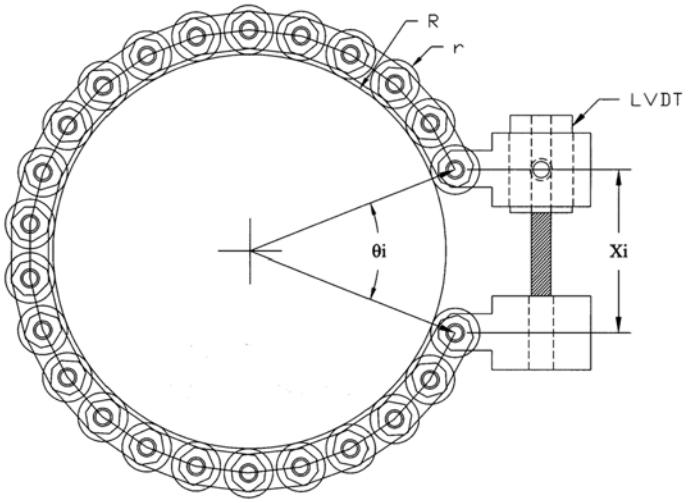

Figure A-1. *Chain for radial deformation measurement.*

Appendix B

This appendix contains results showing the unprocessed data and values on the computed system stiffness K_{system} that were used for the data processing, cf Section 4.4. In addition graphs showing the volumetric strain ε_{vol} versus the axial strain ε_a and the actual radial strain rate $d\varepsilon_r/dt$ versus time are displayed.

Specimen ID: KFM06A-113-21

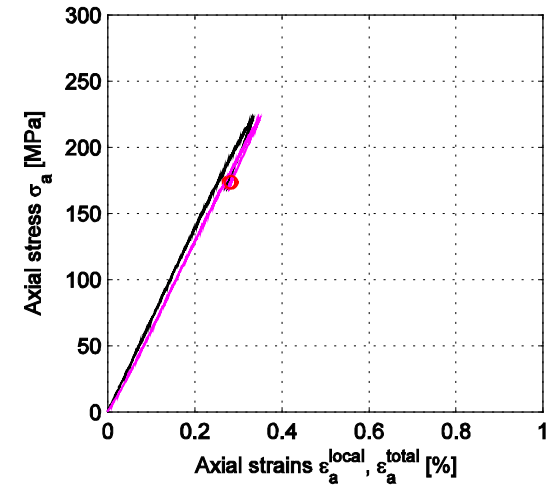

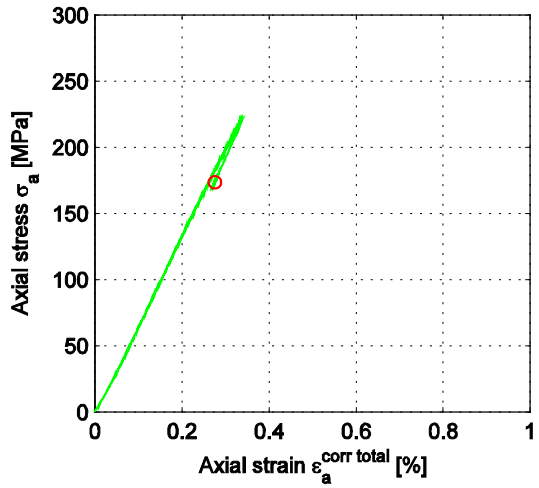

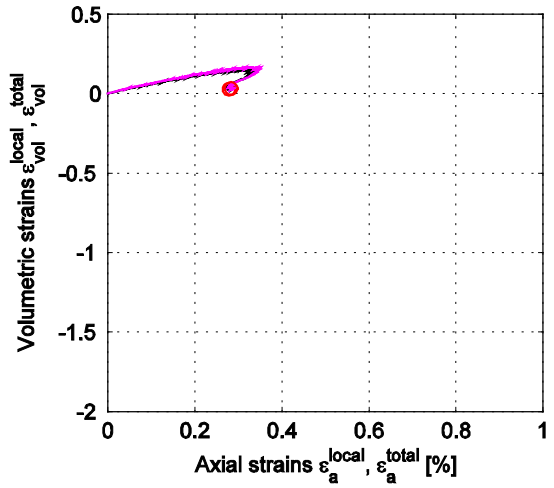

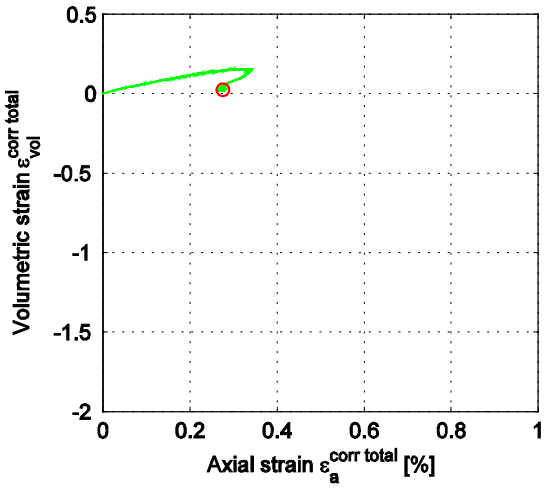

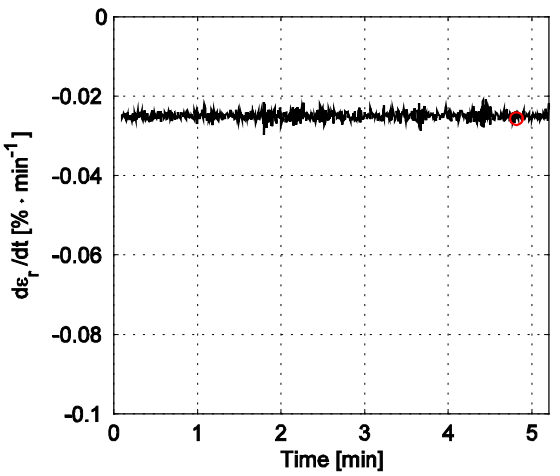

Explanation to curves above:

Based on local deformation (black)

Based on total deformation (magenta)

Based on corrected deformation (green)

Calculated system stiffness:

K_{system} = 34.6 [GN/m]

Specimen ID: KFM06A-113-22

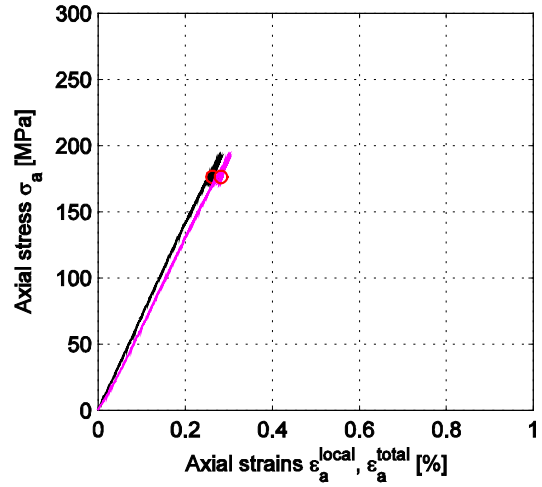

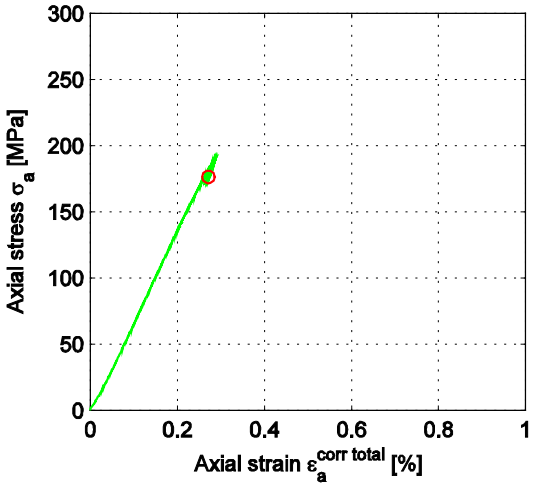

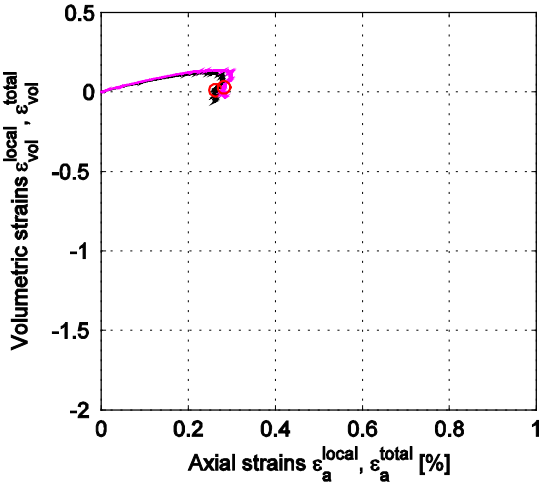

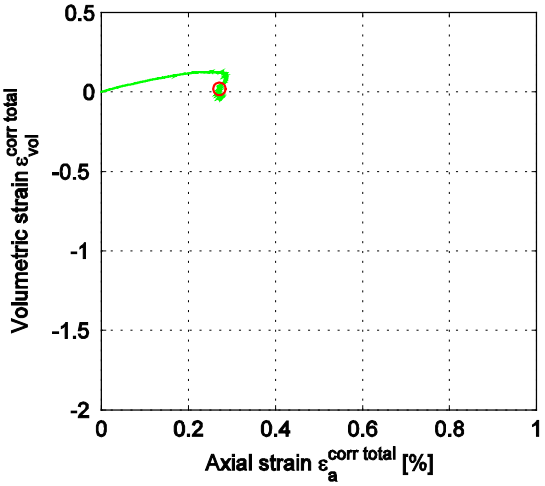

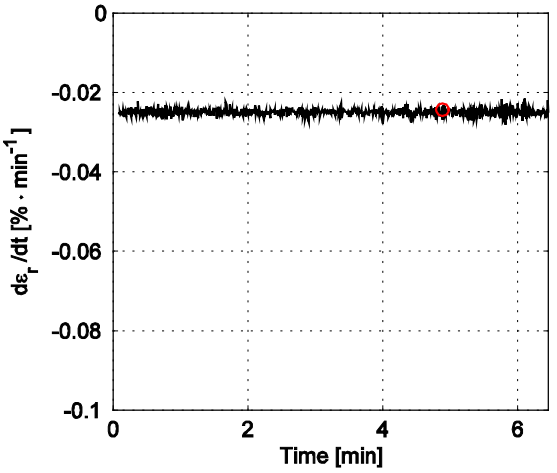

Explanation to curves above:

Based on local deformation (black)

Based on total deformation (magenta)

Based on corrected deformation (green)

Calculated system stiffness:

K_{system} = 25.2 [GN/m]

Specimen ID: KFM06A-113-23

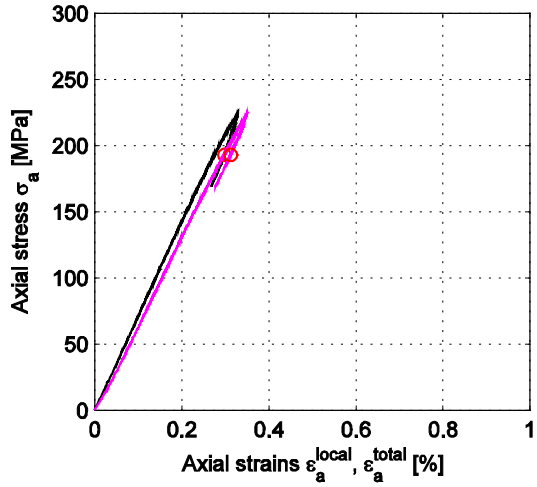

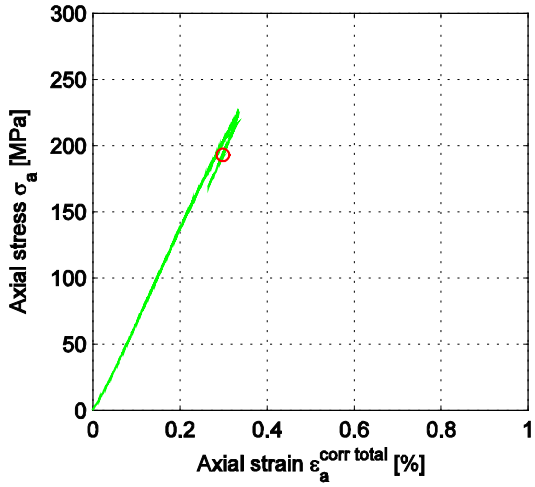

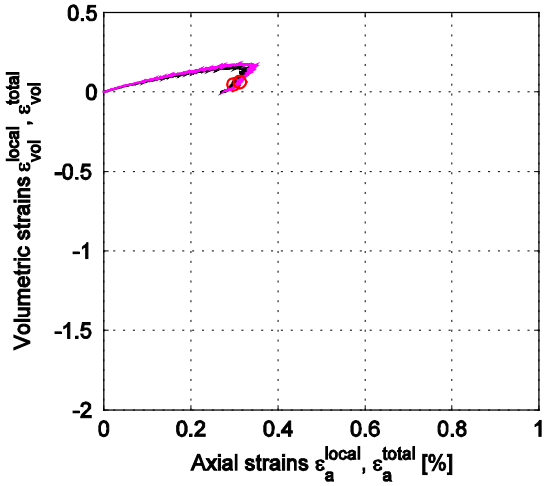

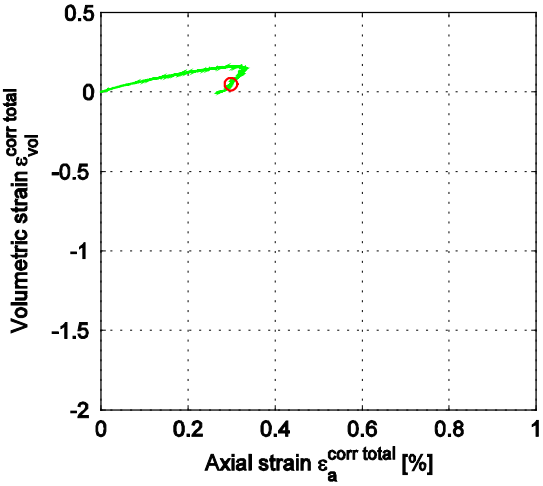

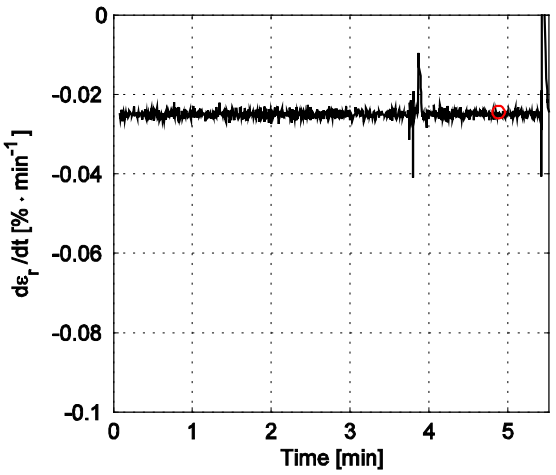

Explanation to curves above:

Based on local deformation (black)

Based on total deformation (magenta)

Based on corrected deformation (green)

Calculated system stiffness:

K_{system} = 22 [GN/m]

Specimen ID: KFM06A-113-24

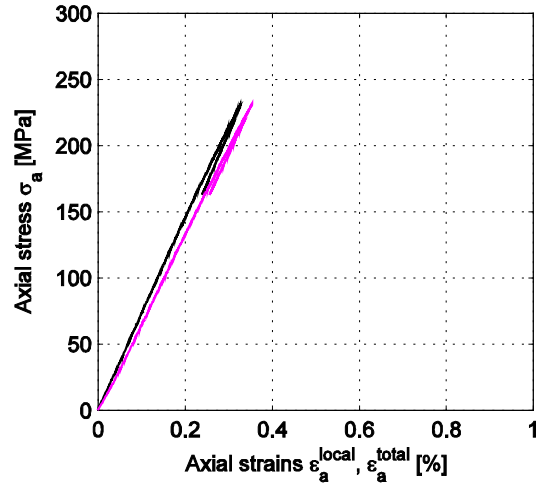

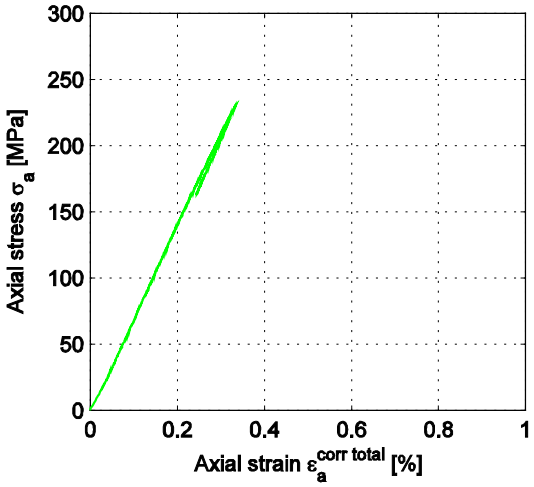

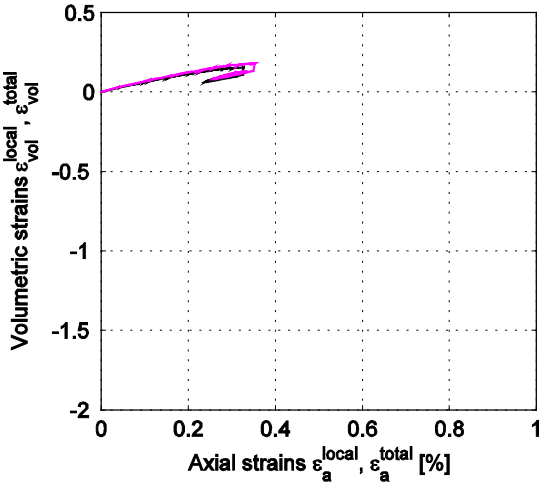

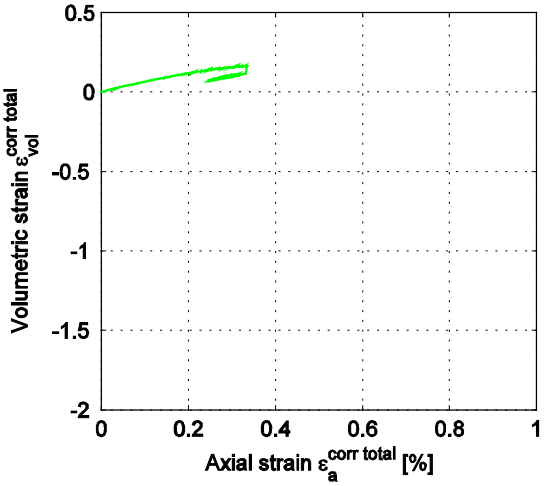

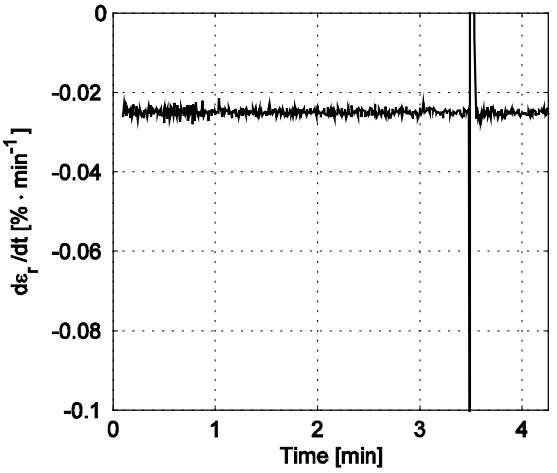

Explanation to curves above:

Based on local deformation (black)

Based on total deformation (magenta)

Based on corrected deformation (green)

Calculated system stiffness:

K_{system} = 19.7 [GN/m]

Specimen ID: KFM06A-113-25

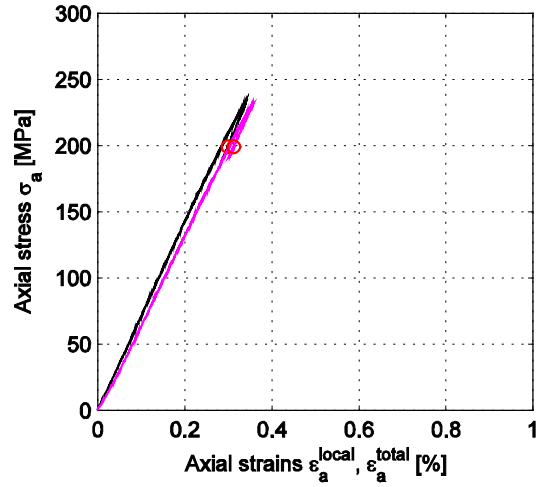

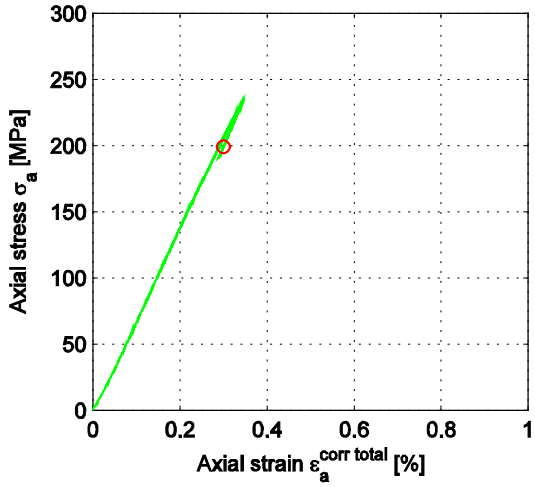

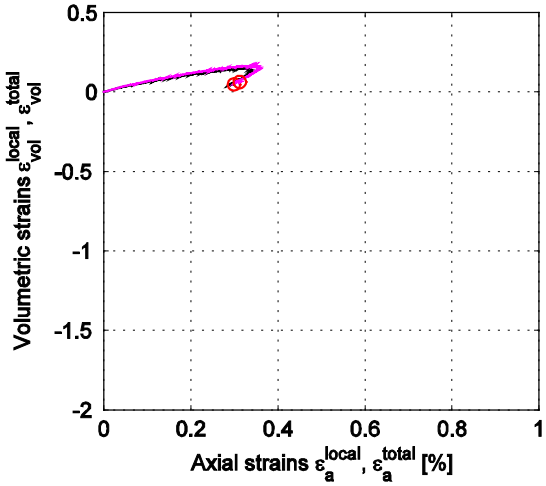

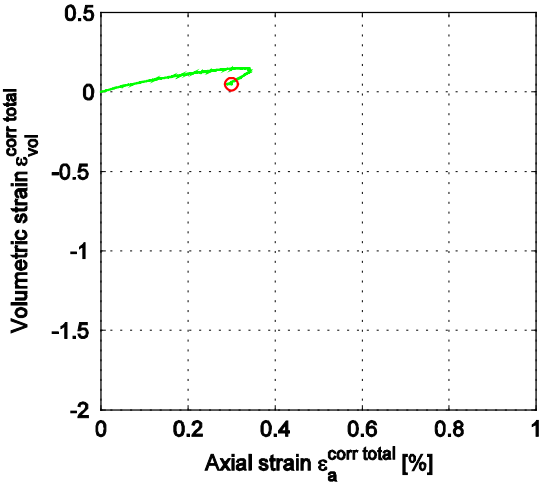

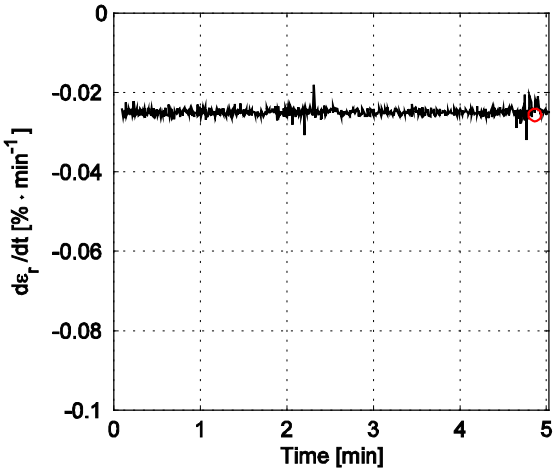

Explanation to curves above:

Based on local deformation (black)

Based on total deformation (magenta)

Based on corrected deformation (green)

Calculated system stiffness:

K_{system} = 25.1 [GN/m]

Specimen ID: KFM06A-113-26

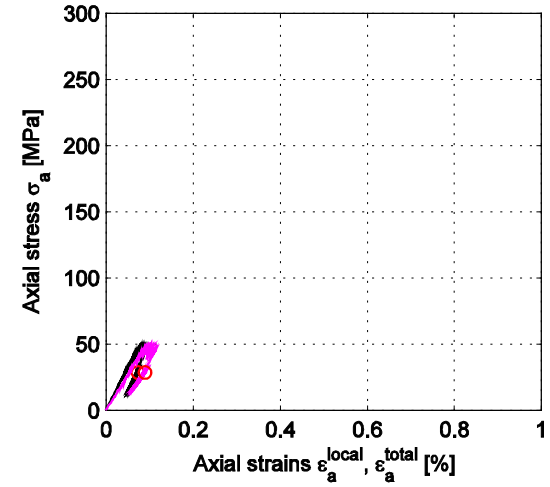

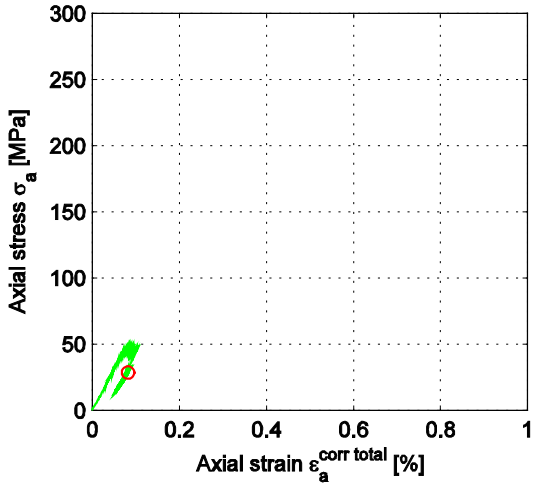

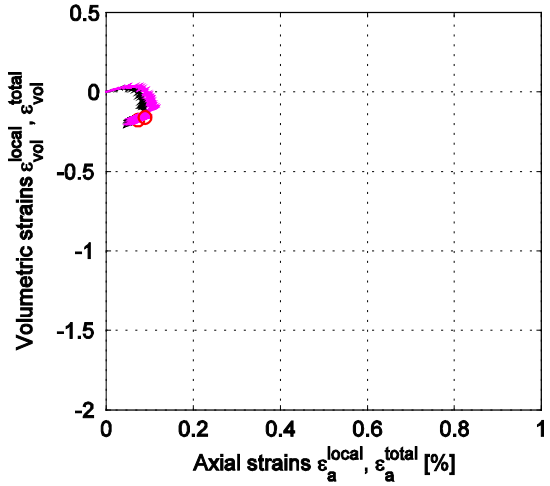

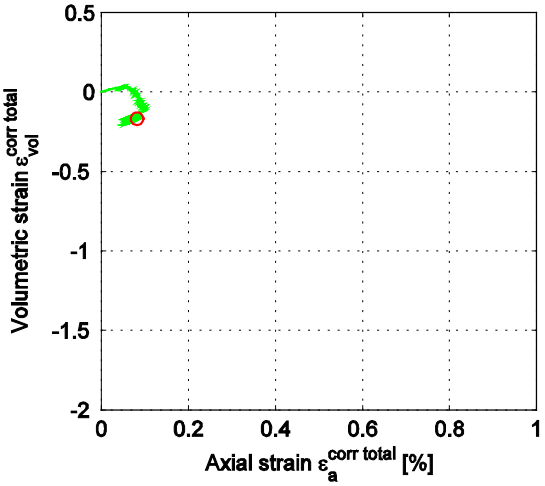

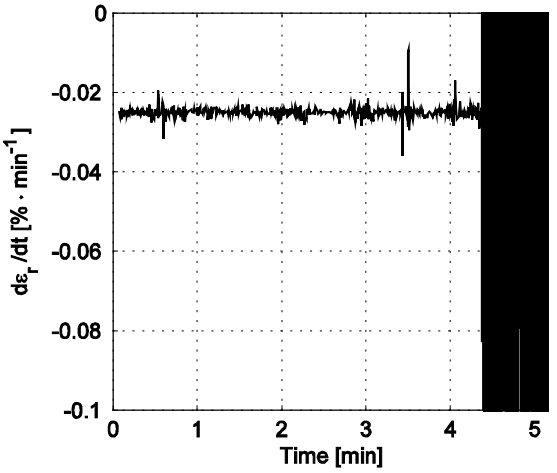

Explanation to curves above:

Based on local deformation (black)

Based on total deformation (magenta)

Based on corrected deformation (green)

Calculated system stiffness:

K_{system} = 6 [GN/m]